IDENTIFICATION OF 1D AND 2D PREISACH MODELS FOR FERROMAGNETS AND SHAPE MEMORY ALLOYS

A. Ktena, D.I. Fotiadis, P.D. Spanos, A. Berger
and C.V. Massalas

8– 2002

Preprint, no 8 – 02 / 2002

Department of Computer Science
University of Ioannina
45110 Ioannina, Greece

Identification of 1D and 2D Preisach models for ferromagnets and shape memory alloys

A. Ktena[1], D. I. Fotiadis[1], P. D. Spanos[2] , A. Berger[3] and C. V. Massalas[4]

[1] Dept. of Computer Science, University of Ioannina, GR 45110 Ioannina, Greece

[2] Dept. of Mechanical Engineering and Materials Science, George R. Brown School of Engineering, Rice University, Houston, USA

[3] IBM, Almaden Research Center, San Jose, CA USA

[4] Dept. of Materials Science, University of Ioannina, GR 45110 Ioannina, Greece

ABSTRACT

A least-squares parameter fitting procedure is used with 1D and 2D formulations of the Preisach formalism. The model can use any operator from a selection of 1D and 2D hysteresis operators appropriate for the modeling of hysteresis in ferromagnets and shape memory alloys. The performance of the hysteresis operators is evaluated and their applicability is discussed. The model is applied to experimental data from ferromagnetic samples and shape memory alloys. The results suggest that the proposed approach can be a useful and adjustable tool in the modeling of hysteresis in various systems regardless of the underlying mechanism.

1 INTRODUCTION

Hysteresis is the non-linear response of a system which, in the context of this work, can be described as a rate independent memory effect [1]: the output is delayed with respect to the input but the input rate does not affect the output state, and the system can store information, i.e. the output depends on the current as well as on previous inputs. One of the approaches in modelling hysteresis is based on the Preisach formalism. The Preisach formalism postulates that hysteresis is the aggregate response of a distribution of elementary hysteresis operators [2]. The resulting model is computationally efficient, and, for systems which fulfill the necessary and sufficient conditions to be modeled by it, reliable [2]. The hysteresis operator of the classical Preisach model (CPM) is a relay (Figs. 1a, 1b) that switches between two states, *e.g.* (+1,-1) or (0,1), at two critical input values, *e.g.* (a,b) where $a > b$. Hence, it is a scalar operator describing only irreversible switching. An extensive discussion on the mathematical properties, the hysteresis operator, the identification and the invert of the CPM can be found in Refs. [1-3].

The inherently scalar nature of the classical model has drawn a considerable amount of criticism on the grounds that the one-dimensional treatment of a hysteresis process is not always valid and a lot of information is lost when modeling the one-dimensional projection of a vector process. Furthermore, the experimental response of a system with hysteresis to an input sequence contains, in general, a reversible component that can be a significant part of the total response. To the extent that the reversible part can be attributed to the reversible rotation of the output vector, one can expect that a vector formulation of the CPM would address both issues. The original

formalism may be extended to two dimensions replacing the operator of Fig. 1a by a 2D operator (Figs. 1d-e) that allows for irreversible switching as well as reversible rotation [4].

Because of the different operator, the 2D model does not have the same properties as the CPM. Hence, some of the theorems and tools accompanying the CPM, as is the case of the identification problem, cannot be applied in the 2D model. In the classical scalar case, the identification of the model consists in the reconstruction of the distribution of the hysteresis operators through a series of detailed measurements [2, 5]. It is not obvious how this method can be applied to two dimensions because of the coupling between the two components of the output. To circumvent this, alternative ways to determine the distribution have been investigated [4, 6].

The method presented in this work is based on the least-squares fitting of the distribution parameters. The only requirement is that, regardless of the underlying mechanism of hysteresis, a major loop measurement of the system or material is available. Even though this method seems, for the time being, to be the only way to identify the 2D model, because of its efficiency, it can also be used with the 1D model. Furthermore, it can be used with a variety of hysteresis operators as long as they are compatible with the Preisach formalism. For example, the Preisach model has originally been designed to model hysteresis in ferromagnets, but can be applied, among others, to elastoplasticity, *e.g.* shape memory alloys (SMA) [7], provided that an appropriate hysteresis operator (Fig. 1b-c) is chosen.

The five operators that can be used with the one- or two- dimensional models and the above mentioned identification method are described in section 2. In Section 3, the performance of the models for the various operators is evaluated and compared for three ferromagnetic samples and an SMA sample.

2 THE MODEL

Scalar operators

In the classical model the operator γ_{ab}, hereafter referred to as "cmp1", is a simple relay with output ±1 and upper and lower switching points a and b, respectively (Fig. 1a). For an input u_t, the output f_t is given by

$$f_t = \gamma_{ab} \circ u_t = \min\{1, f_{t-1}\}, \text{ where } \gamma_{ab} = \begin{cases} +1, & u_t > a \\ -1, & u_t < b \end{cases}. \tag{1}$$

It can be used to model hysteresis in ferromagnets where the output (magnetization) varies between positive and negative saturation and the major loop (Figs. 4-5) is traced in the counterclockwise direction.

The operator in Fig.1b, "cpm2", is a modification of the classical operator and suitable for hysteresis modeling in SMAs where the output (strain) varies between zero and a maximum value and the major loop (Fig. 7) is traced in the clockwise direction:

$$\gamma_{ab} = \begin{cases} 0, & u_t > a \\ +1, & u_t < b \end{cases} \text{ and } f_t = \min\{1, f_{t-1}\}. \tag{2}$$

The operator in Fig.1c, also known as the "kp" operator [7], allows for a linear transition between the minimum and maximum values and bidirectional horizontal movement at any point of the ascending or descending curve. It is appropriate for hysteresis modeling in elastoplasticity, *e.g.* SMAs.

For the descending branch,

$$\gamma_{ab} = \begin{cases} 1 & u_t \le a-\delta \\ \gamma_a & a-\delta < u_t < a+\delta \\ 0 & u_t \ge a+\delta \end{cases}, \qquad \text{where } \gamma_a = 1-\frac{1}{2\delta}\left(u_t - a + \delta\right),$$

and

$$f_t = \min\left\{1, \max\left\{f_{t-1}, \gamma_a\right\}\right\}. \tag{3a}$$

For the ascending branch,

$$\gamma_{ab} = \begin{cases} 0 & u_t \ge b+\delta \\ \gamma_b & b+\delta > u_t > b-\delta \\ 1 & u_t \le b-\delta \end{cases}, \qquad \text{where } \gamma_b = 1-\frac{1}{2\delta}\left(u_t - b + \delta\right),$$

and

$$f_t = \max\left\{0, \min\left\{f_{t-1}, \gamma_b\right\}\right\}, \tag{3b}$$

where 2δ is the difference between the two input values at the beginning and end of the switching process.

A comparison between the responses of the operators, "cpm2" and "kp", for the same input sequence and two δ-values is shown in Fig. 2. The δ-parameter controls the steepness of the ascent (or descent) from 0 to 1 (or from 1 to 0).

Vector operators

The Preisach formulation can be extended to two dimensions using vector 2D operators [4]. The operator of Fig.1d is known as the Stoner-Wohlfarth (sw) astroid and is borrowed from the theory of ferromagnetism. It results from the minimization of the free energy equation of an ellipsoidal magnetic particle with uniaxial anisotropy under an applied field as the locus of equation $u_x^{2/3} + u_y^{2/3} = 1$, where u_x and u_y are the components of the input u along the easy and hard axis of the particle, respectively. The solution ϕ is the angle of the output vector with respect to the easy axis of the astroid: $u_x \tan\phi - u_y + \sin\phi = 0$. It is the tangent to the astroid passing from the tip of the input vector. Switching occurs only if, during the transition from $f(t-1)$ to $f(t)$, the output vector crosses the astroid from the inside out. Otherwise, the output vector rotates reversibly. Because the solution of the transcendental equation can be time consuming, the transformation $k = \tan\frac{\phi}{2}$ and the roots of the resulting equation: $u_y k^4 + 2(u_x - 1)k^3 + 2(u_x + 1)u - u_y = 0$ can be used instead. Then, $f_x = \cos\phi$ and $f_y = \sin\phi$.

The second vector operator (Fig. 1e), the diamond (dm), is the first order approximation of the sw-astroid: $u_x + u_y = 1$ and uses a similar hysteresis mechanism. It is computationally more efficient but it does not have any physical attributes. Both vector operators are used for hysteresis modeling in ferromagnets. For inputs along the x-direction, the vector operators respond identically to the classical scalar operator of Fig. 1a.

A comparison between the two 2D operators is shown in Fig. 3. The output is calculated for rotating inputs of constant magnitude. For very small inputs, the response is practically identical. As the input increases but not enough to cause switching, the sw-astroid rotates harder than the diamond. For large inputs, the sw-astroid allows for more switching.

Modeling the hysteresis process

In the Preisach approach, the parameters a and b of the hysteresis operators are distributed according to a probability density function $\rho(a,b)$ over a half-plane, called the Preisach plane, that is defined by $a \geq b$. The hysteresis process is then modeled as the aggregate response of the distributed operators to a sequence of inputs. The output $f(t)$ is then given by

$$f(t) = \iint_{a \geq b} \rho(a,b)\gamma_{ab} \circ u(t) da db . \tag{4}$$

Using a 2D-operator γ_{ab} instead of (4) describes a 2D-model for a perfectly oriented (po) system, i.e. all the easy axes of the operators lie along the same orientation direction. However, actual systems, as a rule, are not perfectly oriented and the question of orientation dispersion needs to be addressed. Systems that are not perfectly oriented can be modeled by

$$f(t) = \int_{-\pi/2}^{\pi/2} \rho(\theta) d\theta \iint_{a \geq b} \rho(a,b)\gamma_{ab} \circ \boldsymbol{u}(t) da db , \tag{5}$$

where $\rho(\theta)$ is the probability density function of the angles that the easy axes of the 2D operators γ_{ab} form with the model's axis of orientation [4]. Fig. 4 shows calculated major loops obtained by the model of Eq. (4) and the operators "cpm1",

"sw", and "dm" (the perfectly oriented case) and the model of (5) using the two vector operators "sw" and "dm". The scalar and perfectly oriented models yield identical results for fields along the model's easy axis, as expected. Adding dispersion makes switching easier, which is in agreement with experimental evidence in ferromagnets, and accounts for the reversible behavior and the slope of the curve at the remanent state, $f(u=0)$. Note that the model using the "sw" predicts narrower loops than the one using the "dm". This is in agreement with the previous remark that the "sw" allows for more switching.

The density $\rho(a,b)$

In order to identify a Preisach-type model for a given system, its characteristic density $\rho(a,b)$ must be determined. Using the transformation, $a=\frac{c-d}{\sqrt{2}}$ and $b=-\frac{c+d}{\sqrt{2}}$, the density can also be determined in terms of the variables c and d: $\rho(a,b)=\rho(c,d)$. It can be shown that, if c and d are independent, the following relationships apply:

$$\rho(a,b)=\rho(c,d)=\rho(c)\rho(d), \tag{6a}$$

$$E[c]E[d]=\frac{1}{2}\left(E[b]^2-E[a]^2\right) \text{ and } E[d]=0, \tag{6b}$$

$$Var[a]=Var[b]=\frac{1}{2}\cdot\left(Var[c]+Var[d]\right), \tag{6c}$$

where $E[\,]$ and $Var[\,]$ are the expectation and the variance respectively of a parameter. It follows that $E[a]=-E[b]$ and $Var[a]=Var[b]$. In that case, the loops obtained are symmetric like the ones shown in Fig. 4: $f(-u)=-f(u)$.

In the case of ferromagnets, $\rho(c)$ and $\rho(d)$ are related to the distribution of coercivities and interactions, respectively, and it is valid to assume that the

coercivities and interactions are uncorrelated and that the mean interaction field is zero [4,6].

In the case of the classical model of Eq. (4), the density $\rho(a,b)$ can be determined experimentally using the Everett functions [5, 2]. However, in the 2D model of Eq. (5), it is not obvious how the effect of the transverse and longitudinal components on the distribution can be decoupled and determined experimentally. In this case, Eq. (6a) can be utilized and the density can be reconstructed as the product of two independent single-variable densities. $\rho(c)$ and $\rho(d)$ can then be modeled by standard probability density functions (Gaussians, Lorentzians). The parameters of the densities are fitted using major loop data [4,8]. This method will be referred to as "old".

The "new" method, used in this work, is using a Gaussian $N(\mu,\sigma^2)$ to model the original density $\rho(a,b)$ and a least-squares fitting procedure to determine its parameters [8]. An array of i points of the experimental major loop is fed to the least squares algorithm along with an array of initial estimates of the parameters and the algorithm iterates on the parameter values until $\sum_i \left(f_{\text{mod}} - f_{\text{exp}}\right)^2 < \varepsilon$, where ε is a small positive number.

3 RESULTS AND DISCUSSION

To evaluate the performance of the models and the operators discussed in section 2 in relation with the identification method proposed, major loop data from three

ferromagnetic samples and an SMA sample have been modeled. In ferromagnets, hysteresis occurs during the switching from positive to negative magnetization and the opposite. For an applied magnetic field (input) $H(t)$, the resulting magnetization (output) is a function of the applied field as well as an internal interaction field, which is in turn a function of the magnetization $M(t)$. Hence, the resulting magnetization state contains a positive feedback mechanism leading to hysteresis: $M(t) = M(H(t), M(t))$. In shape memory alloys, hysteresis can be observed as the material undergoes the transformation from the martensitic to the austenitic phase and vice versa. The input is the temperature, $T(t)$, and the output is the strain $x(t)$ [7].

The ferromagnetic case

The ferromagnetic data has been modeled using the 1D-model of Eq. (4) with the operator "cpm1" of Eq. (1), and the 2D-model of Eq. (5) with the vector operators "sw" and "dm". Because of the observed symmetry of the loops in ferromagnets $\mu_a = \mu_b = \mu$ and $\sigma_a = \sigma_b = \sigma$. If the Preisach plane is modeled as a $K \times K$ array, the initial estimates for the parameters are given by $\hat{\mu}_a = \hat{\mu}_b = \frac{K}{2} + H_c$ and $\hat{\sigma}_a = \hat{\sigma}_b = \frac{\left(\frac{K}{2} - H_c\right)}{3}$, where $\hat{\mu}_a$, $\hat{\mu}_b$, $\hat{\sigma}_a$, $\hat{\sigma}_b$ are the initial estimates for the mean values, μ, and standard deviations, σ, of a and b. H_c is the measured coercivity of the magnet, defined as the field at which the magnetization is zero, $M\big|_{H_c} = 0$.

Table 1 summarizes the results of the least squares fitting procedure for the first sample, SmFeN, with coercivity H_c=15 kOe. Table 2 shows the results for the second sample, α-Fe/SmFeN, with coercivity H_c=3 kOe.

Table 1: The SmFeN parameters

	cpm1	sw	dm
K	70	60	60
μ	49.859	51.132	43.223
σ	5.721	4.007	2.216

Table 2: The α-Fe/SmFeN parameters

	cpm1	sw	dm
K	30	70	50
μ	19.651	40.831	29.210
σ	2.915	2.872	2.971

Figs. 5 and 6 show the major loop curves generated by the 1D- and 2D- models and operators using the parameters of Tables 1 and 2, respectively. They are compared against the corresponding measured curve and a calculated curve generated by the 2D-model using the "old" identification procedure. The magnetization, M, is normalized to the saturation magnetization M_s. In both cases, the results are consistent. The "new" identification procedure is more accurate and the 2D-model is superior to the 1D-model at the region of the remanence, $M_r = M\big|_{H=0}$, where most of the reversible processes take place. The fitting of the curve obtained using the "sw" operator is as good (α-Fe/SmFeN) or worse (SmFeN) than the "dm"-curve and is not shown here. The "dm" routine is more efficient than the "sw" routine, so, unless the

"sw"-operator performs better than the "dm" the latter is preferred. In the case of the α-Fe/SmFeN sample (Fig. 6), the fitting is excellent. On the other hand, the SmFeN loop is very steep around the coercivity, *i.e.* it has a high coercivity squareness, $S^* = \left.\frac{dM}{dH}\right|_{H_c}$, but it is not square at the remanence, *i.e.* it has a low squareness ratio, $S = \frac{M_r}{M_s}$. Therefore, the rotational properties of the 2D-model are needed around the remanence but the switching properties of the classical operator would be desirable around the coercivity. The optimum choice, as shown in Fig. 5, is the 2D-model with the "dm" operator but it leaves room for improvement. A possible alternative is to use the least-squares fitting of the parameters along with Eq. (6a) and a Lorentzian instead of a Gaussian for the interactions distribution, $\rho(d)$.

Table 3 summarizes the parameter values obtained for the descending curves of a thin film sample measured at 610 °C and 560 °C. The temperature dependence of the magnetic properties and the microstructure is reflected in the phenomenology of the curves. As seen in Fig. 7, the 610 °C curve is accurately reproduced by the 1D-model using the classical operator (cpm1) and the 560 °C curve by the 2D-model and the 'sw' operator. As expected, for square loops like the 610 °C curve the classical 1D model can be very accurate and the high S^* of the curve is reflected in the low σ-value obtained. As the temperature decreases, the loops become less square both at the remanence and the coercivity and the 2D model is needed. For low S^* loops, like the 560 °C curve, the sw-astroid performs better.

Table 3: The thin film sample parameters

T (°C)	560	610
model	2D/sw	1D/cpm1
K	60	40
μ	51.439	25.827
σ	2.798	0.480

The SMA case

In this case, the input variable is temperature and the output variable is deformation (strain). The SMA data are modeled using the 1D model of Eq. (4) and the hysteresis operators "cpm2" (Fig. 1b) and "kp" (Fig. 1c) described by Eqs. (2) and (3), respectively. SMA loops are traced in the opposite direction compared to magnetic loops. The ascending branch is the one to the left and is traced as the temperature decreases. The output is normalized to the maximum % strain observed and ranges from 0 to 1. Unlike the case of ferromagnets, the loop is not symmetric but skewed and shifted to the right with respect to the origin. This suggests that $\mu_b > \mu_a$ and $\sigma_b > \sigma_a$.

Let T_a be the temperature at which the normalized % strain has reached 0.5 on the ascending branch (martensite to austenite) and T_m the temperature at which the normalized % strain has reached 0.5 on the descending branch (austenite to martensite). The initial estimates used in the identification algorithm are:

$$\hat{\mu}_a = \frac{K}{2} - T_m \ , \ \hat{\mu}_b = \frac{K}{2} - T_a \ , \ \hat{\sigma}_a = \frac{\frac{K}{2} - T_m}{3} \ , \ \hat{\sigma}_b = \frac{\frac{K}{2} - T_a}{3} \ .$$

Table 4 summarizes the least-squares fitting results for the density parameters used in the modeling of the SMA curves. Fig. 8 shows major and minor loops obtained using the two operators "cpm2" and "kp" against the corresponding experimental curves obtained on a Nitinol sample, with $T_a = 0$ and $T_m = 20$. The δ-parameter in Eq. (1c) depends on the loop width of the operator: $\delta = k(a-b)$, $k < 1$. For the results shown in Fig. 7, $k=0.6$.

Table 4: The SMA parameters

	cpm2	kp
K	81	81
μ_a	20.401	20.386
σ_a	7.726	5.016
μ_b	40.339	38.889
σ_b	11.377	10.960

The loops that were calculated using the "kp" operator are closer to the experimental data. Note also that the σ-values obtained for "cpm2" are higher than "cmp3". It is important to note that the minor loops are also adequately reproduced by the model, even though the data used for the identification were taken from the major loop curve only. The use of minor loop points did not provide any improvement to the fitting of the curves while it considerably increased the time for the least-squares computation. The discrepancies observed are due rather to the shape of the distribution than the choice of operator.

The model, the operators and the identification procedure were all implemented in MATLAB 5.0. A major loop calculation for 100 input values would need

approximately between 0.5 and 5 minutes on a Celeron PC at 330Hz. The efficiency of the computation depends on the choice of operator and the dimensionality of the model, e.g. the 1D model with "cpm1" or "cpm2" is the most efficient routine while the 2D model using the "sw" operator results in the lengthiest calculation.

4 CONCLUSIONS

The proposed model in the 1D and 2D version equipped with a selection of 1D and 2D operators and an identification method based on a least squares fitting of the density parameters can be a handy tool in the reproduction of hysteresis processes. It can model efficiently a variety of hysteresis loops, regardless of the microstructure of the material or the mechanism of hysteresis, as long as the appropriate operator is chosen. The identification method relies on a mere major loop measurement, a feature that makes it attractive even for use with the 1D model.

More specifically, the 1D model using the classical operator is appropriate for square loops. In the case of ferromagnets, for loops with lower squareness values, it is necessary to use the 2D-model along with a vector operator to account for the effect of the rotation of the magnetization vectors. Loops with low coercivity squareness are better modeled by the "sw" operator. The "kp" operator is appropriate for the modeling of hysteresis in SMAs even though the normal distribution may not be the best choice. The choice of the shape of the distribution is still an open question.

Acknowledgements

The authors would like to thank Prof. Lagoudas of the Department of Aerospace Engineering, Texas A&M University, for kindly providing the SMA hysteresis data used in this work.

References

1. A. Visintin, in: Differential Models of Hysteresis, 10-29, Springer, Berlin (1994).
2. I. D. Mayergoyz, Mathematical models of hysteresis, Physical Review Letters, 56(15), 1518-1521 (1986).
3. M. Brokate and J. Sprekels in: Hysteresis and Phase Transitions, 93-121, Springer, Berlin (1996).
4. S. H. Charap and A. Ktena, Vector Preisach modeling, J. Appl. Phys., 73, 5818-5823 (1993).
5. D. H. Everett, A general approach to hysteresis, Trans. Faraday. Soc., 51, 1551-1557 (1955).
6. A. Ktena and S. H. Charap, Vector Preisach Modeling and Recording Applications, IEEE Trans. Magn., 29 (6), 3661-3663 (1993).
7. Z. Bo, et. al., Int. J. Eng. Sci. 37, 1205 (1999).
8. A. Ktena, D.I. Fotiadis and C.V. Massalas, IEEE Trans. Mag., New 2-D model for inhomogeneous permanent magnets, 36(6), 3926-3931 (2000).
9. A. Ktena, D.I. Fotiadis, P.D. Spanos and C.V. Massalas, A Preisach model identification procedure and simulation of hysteresis in ferromagnets and shape-memory alloys, Phys. B, 306(1-4), 84-90 (2001).

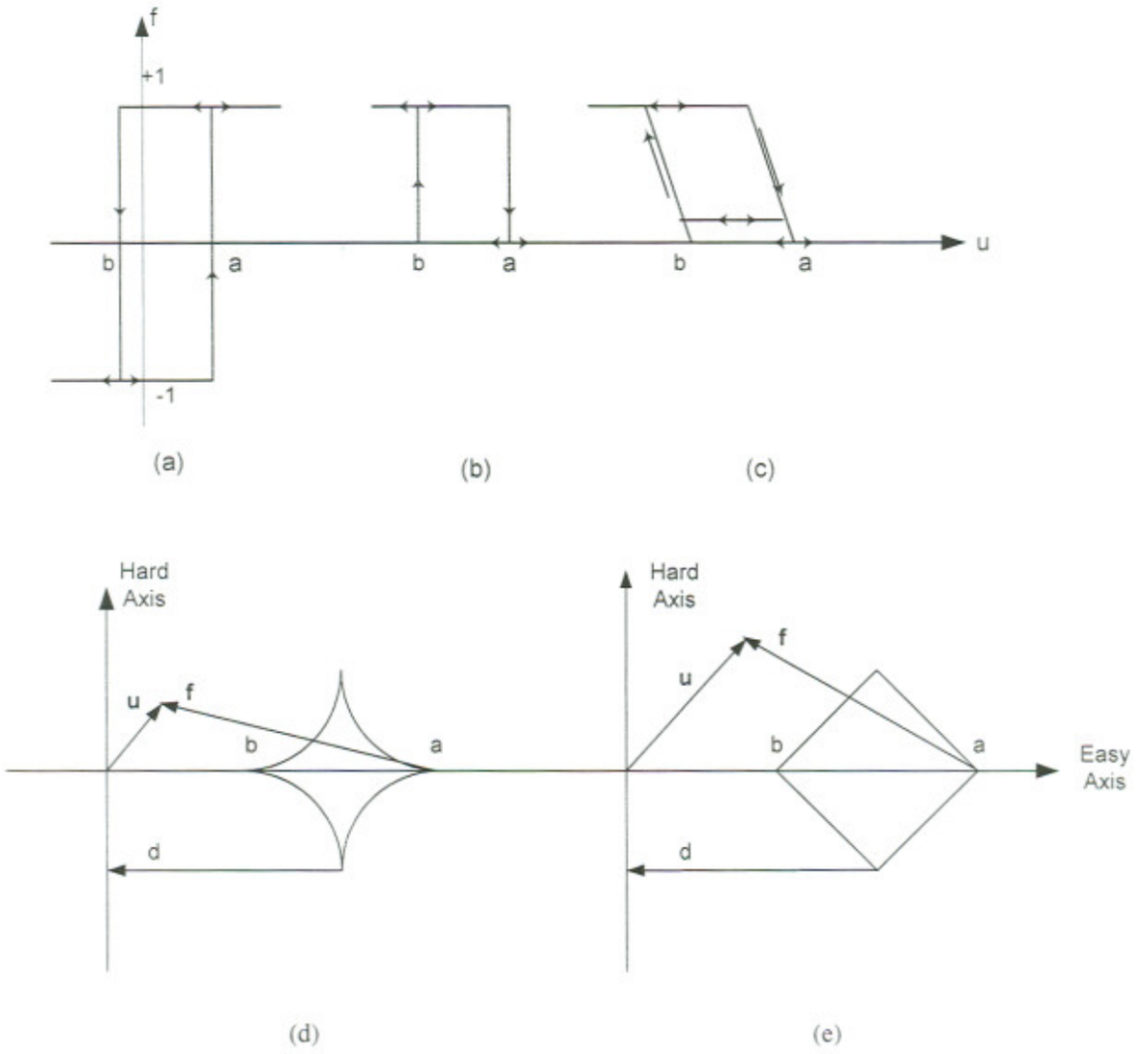

Figure 1: Hysteresis operators: (a) cpm1, (b) cpm2, (c) kp, (d) sw, and (e) dm.

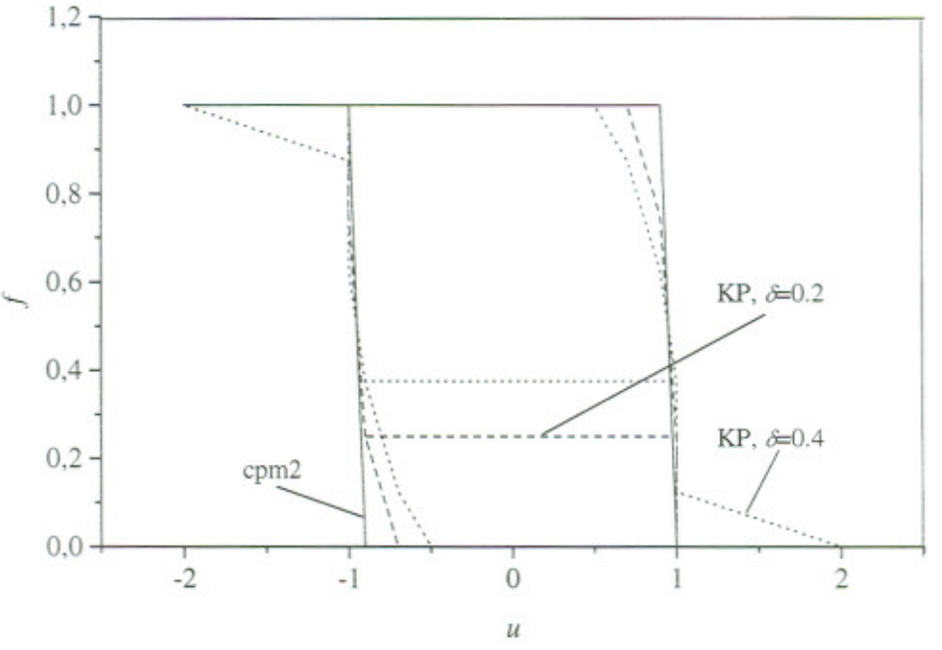

Figure 2: Comparison between the operators "cpm2" and "kp"

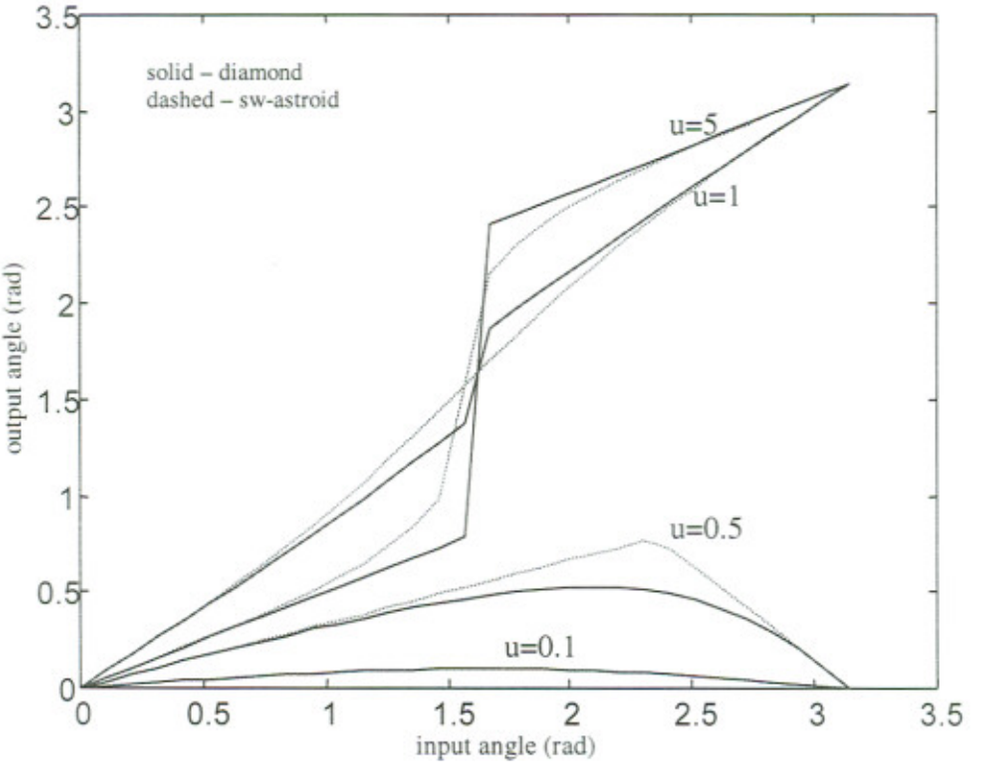

Figure 3: Comparison between the operators 'dm' and 'sw':
An input of constant magnitude, u=0.1, 0.5, 1, 5, is rotated 2π rad.

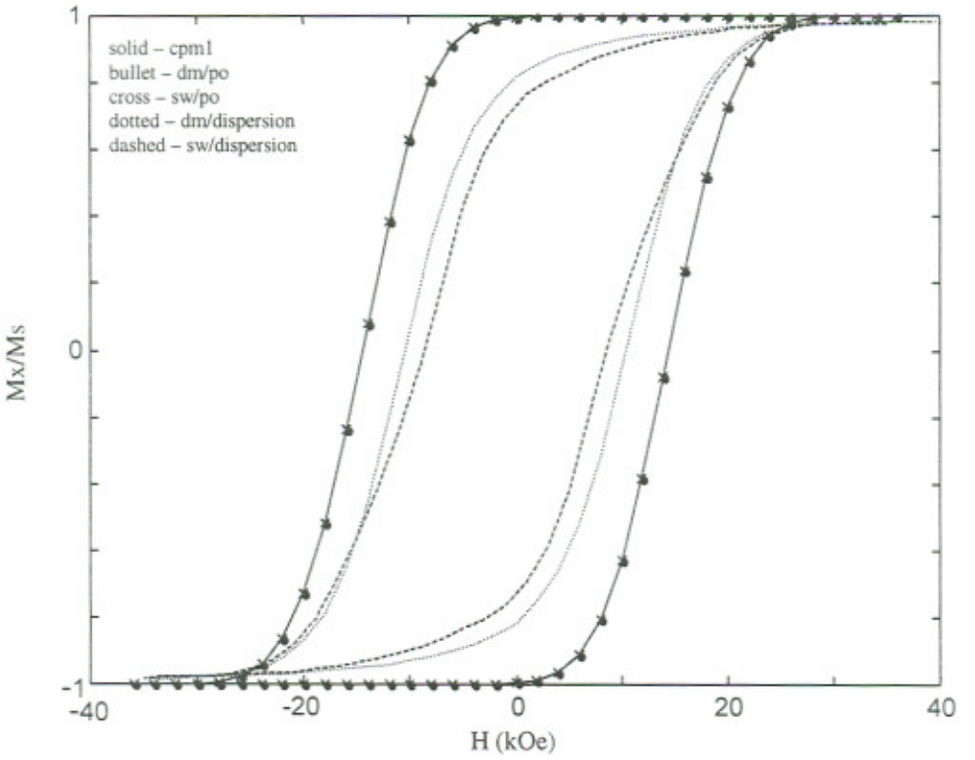

Figure 4: Calculated major loops using three different operators – The effect of dispersion.

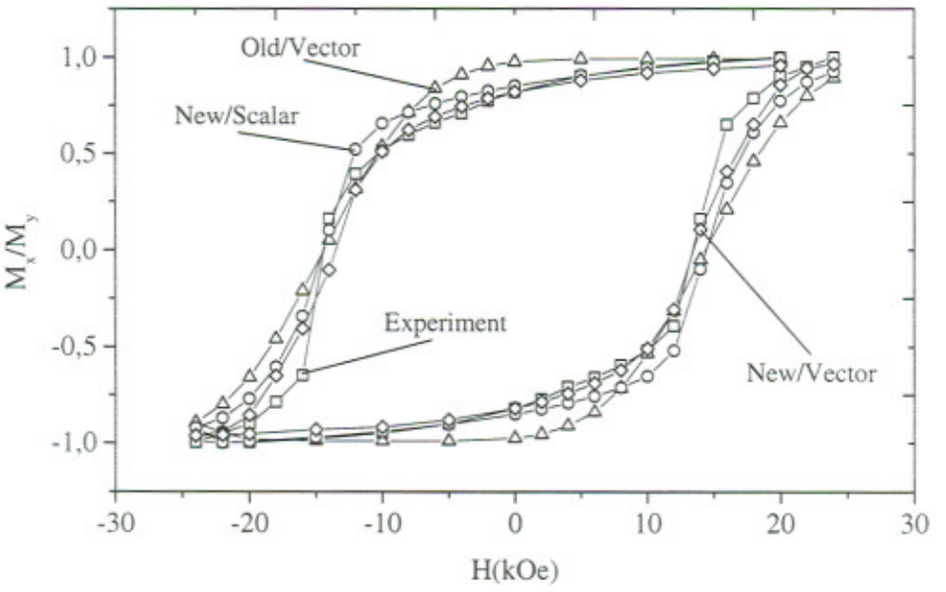

Figure 5: SmFeN experimental and calculated curves.

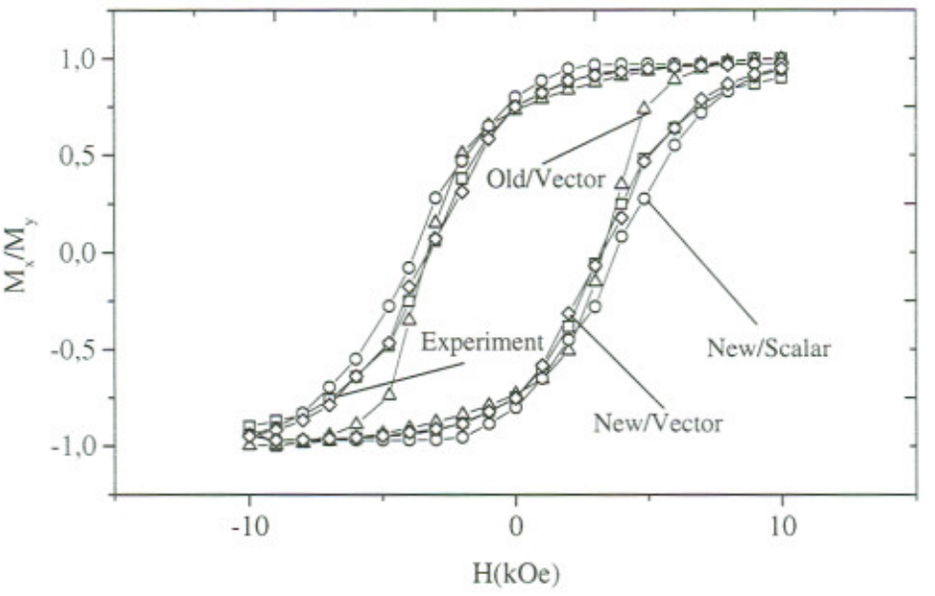

Figure 6: SmFeN/α-Fe experimental and calculated curves.

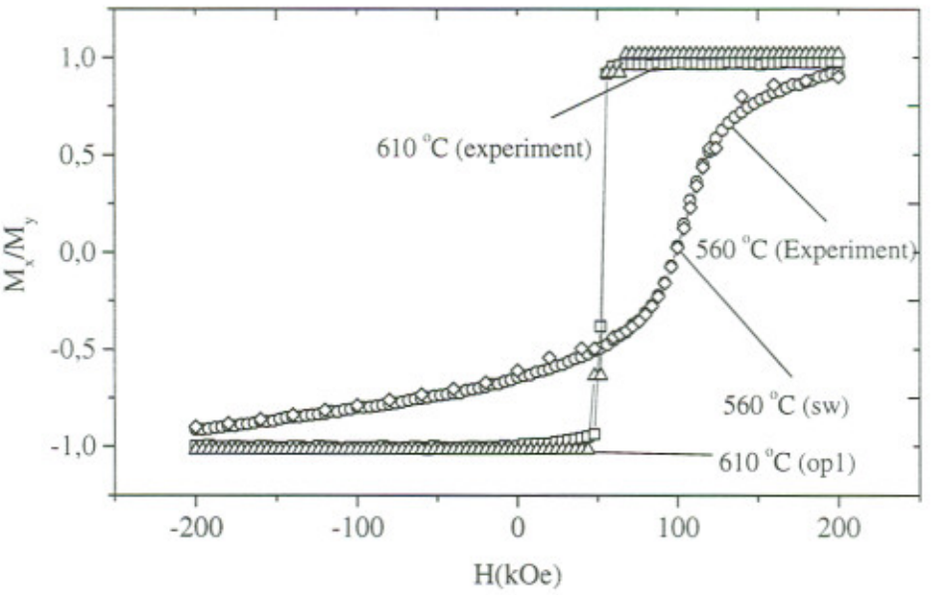

Figure 7: Thin film: experimental and calculated descending curves.

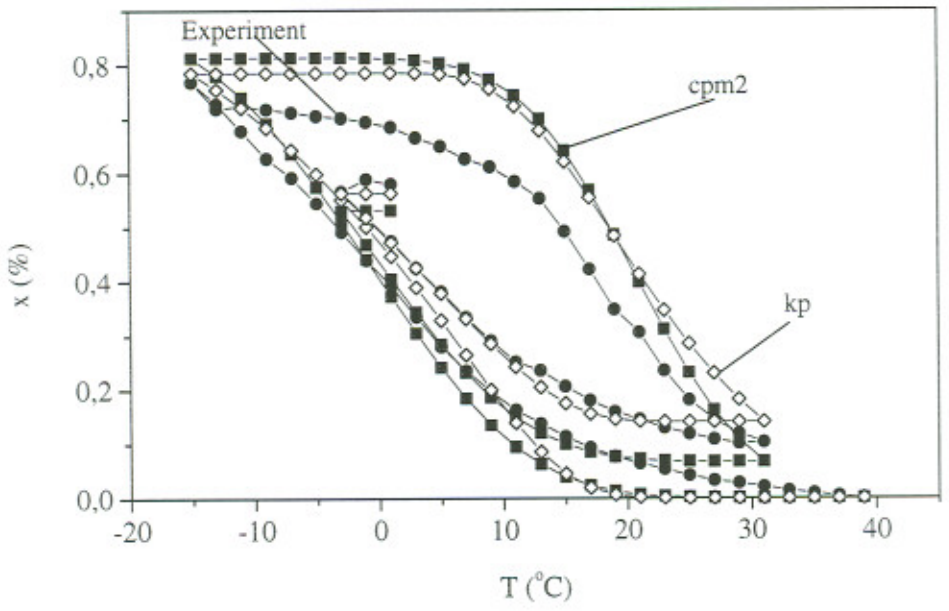

Figure 8: Nitinol: Experimental and calculated major and minor loops.